NKS-371
ISBN 978-87-7893-456-7

ATR-2 Part A: Ruthenium chemistry and transport in a RCS due to air radiolysis products

Ivan Kajan[1]
Teemu Kärkelä[2]
Ari Auvinen[2]
Christian Ekberg[1]

1 Chalmers University of Technology, Sweden
2 VTT Technical Research Centre of Finland

July 2016

Abstract

In the NKS-R ATR-2 activity (year 2015) by VTT Technical Research Centre of Finland Ltd and Chalmers University of Technology, Sweden the aim was to study the effect of the air radiolysis products N_2O, NO_2, HNO_3 (see Part A) and CsI aerosol (see Part B) on the transport of gaseous and particulate ruthenium species through a model primary circuit. The outcomes of the air radiolysis products impact on Ru behaviour are summarized in this report (Part A).

All the experiments were conducted with VTT´s Ru transport facility. The RuO_2 precursor was heated inside a furnace up to 1300 K, 1500 K and 1700 K under slightly humid air atmosphere and the formation of gaseous ruthenium oxides took place. The air radiolysis products N_2O, NO_2 and HNO_3 were fed into the flow of ruthenium oxides. In the experiments nitrogen oxides as well as nitric acid originating from air radiolysis, which is an inevitable phenomenon during a severe nuclear accident, had a significant effect on the ruthenium chemistry in the model primary circuit. The fraction of transported gaseous ruthenium was increased when NO_2 or HNO_3 was injected into the air-flow with volatile ruthenium oxides. This effect was most prominent in case of NO_2 precursor at temperature of 1300 K. The overall transport of ruthenium was strongly increased at 1500 K when N_2O was injected into the gas phase, when compared to the pure humid air atmosphere.

The obtained results indicate a strong effect of air radiolysis products on the quantity of transported ruthenium and its partition to gaseous and aerosol compounds.

Key words

Ruthenium, Radiolysis, Nitrogen oxides, Severe Accident, Source Term

NKS-371
ISBN 978-87-7893-456-7
Electronic report, July 2016

NKS Secretariat
P.O. Box 49
DK - 4000 Roskilde, Denmark
Phone +45 4677 4041
www.nks.org
e-mail nks@nks.org

ATR-2 Part A: Ruthenium chemistry and transport in a RCS due to air radiolysis products

Research Report of the NKS-R ATR-2 activity

(Contract: AFT/NKS-R(15)111/2)

Ivan Kajan[1], Teemu Kärkelä[2], Ari Auvinen[2], Christian Ekberg[1]

[1] Chalmers University of Technology, SE-41296 Göteborg, Sweden

[2] VTT Technical Research Centre of Finland Ltd, FI-02044 Espoo, Finland

June 2016

Report's title	
ATR-2 Part A: Ruthenium chemistry and transport in a RCS due to air radiolysis products	
Customer, contact person, address NKS-R, Programme Manager Karin Andgren, VATTENFALL, SE-169 92 Stockholm, Sweden	Order reference AFT/NKS-R(15)111/2
Project name Impact of Aerosols on the Transport of Ruthenium in the primary circuit of nuclear power plant	Project number/Short ATR-2
Author(s) Ivan Kajan, Teemu Kärkelä, Ari Auvinen, Christian Ekberg	Pages 25
Keywords Ruthenium, Radiolysis, Nitrogen oxides, Severe Accident, Source Term	Report identification code

Summary

In the NKS-R ATR-2 activity (year 2015) by VTT Technical Research Centre of Finland Ltd and Chalmers University of Technology the aim was to study the effect of air radiolysis products N_2O, NO_2, HNO_3 (see Part A) and CsI aerosol (see Part B) on the transport of gaseous and particulate ruthenium species through a model primary circuit. The outcomes of the air radiolysis products impact on Ru behavior are summarized in this report (Part A).

All experiments were conducted with VTT´s Ru transport facility. The RuO_2 precursor was heated inside a furnace up to 1300 K, 1500 K and 1700 K under slightly humid air atmosphere and the formation of gaseous ruthenium oxides took place. The air radiolysis products N_2O, NO_2 and HNO_3 were fed into the flow of ruthenium oxides. In the experiments nitrogen oxides as well as nitric acid originating from air radiolysis, which is an inevitable phenomenon during a severe nuclear accident, had a significant effect on the ruthenium chemistry in the model primary circuit. The fraction of transported gaseous ruthenium was increased when NO_2 or HNO_3 was injected into the air-flow with volatile ruthenium oxides. This effect was most prominent in case of NO_2 precursor at temperature of 1300 K. The overall transport of ruthenium was strongly increased at 1500 K when N_2O was injected into the gas phase, when compared to the pure humid air atmosphere.

The obtained results indicate a strong effect of air radiolysis products on the quantity of transported ruthenium and its partition to gaseous and aerosol compounds.

Confidentiality	Public

Espoo, 28.06.2016

Ari Auvinen,
Principal Scientist, Coordinator of Activity

Contact address

VTT Technical Research Centre of Finland Ltd, Biologinkuja 7, FI-02044 VTT, Espoo, Finland

Chalmers University of Technology, Kemivägen 4, SE-41296 Göteborg, Sweden

Preface

The experiments on the transport of Ru in primary circuit conditions were conducted at VTT Technical Research Centre of Finland Ltd (Espoo, Finland) in 2015. The "VTT's Ru transport facility" was slightly updated for these new experiments. The samples of gaseous and particulate ruthenium, produced as a result of experiments, were analysed with various techniques at Chalmers University of Technology (Göteborg, Sweden) and VTT (Espoo, Finland). The activation of Ru samples for INAA analysis was performed with VTT´s research reactor.

The work was funded by NKS, SAFIR2018 and APRI9 programmes.

Espoo, 28.06.2016

Authors

NKS conveys its gratitude to all organizations and persons who by means of financial support or contributions in kind have made the work presented in this report possible.

Table of Contents

1. Introduction

During a nuclear accident the most important chemical elements are those forming volatile compounds that can be released from the irradiated fuel into the environment. Among others ruthenium is one of the critical radiotoxic elements in the case of an accident due to its ability to form volatile oxides in oxidizing conditions. Ruthenium oxides can be then readily released from the fuel. This can cause a health risk for the personnel of nuclear power plant, as well as for population in general in case of a release to the environment.

For a proper evaluation of the possible source term during an accident, the quantity of the released radioactive nuclides and their transport and further interactions with the structural materials in the nuclear power plant are necessary to be known. The release of fission products from irradiated nuclear fuel samples under different experimental conditions was investigated within the PHÉBUS FP and VERCORS research programs [1-3]. It was shown that depending on the conditions up to 17 % of ruthenium content in the burned fuel can be released under oxidizing conditions [1]. The release rate of ruthenium was strongly dependent on the partial pressure of oxygen in the atmosphere and on the temperature of the fuel [2, 3]. Based on thermodynamic equilibrium calculations with the Factsage thermochemical software, ruthenium will be released from the fuel mainly in form of gaseous RuO_2, RuO_3 and RuO_4 depending on the temperature as can be seen in Figure 1[4].

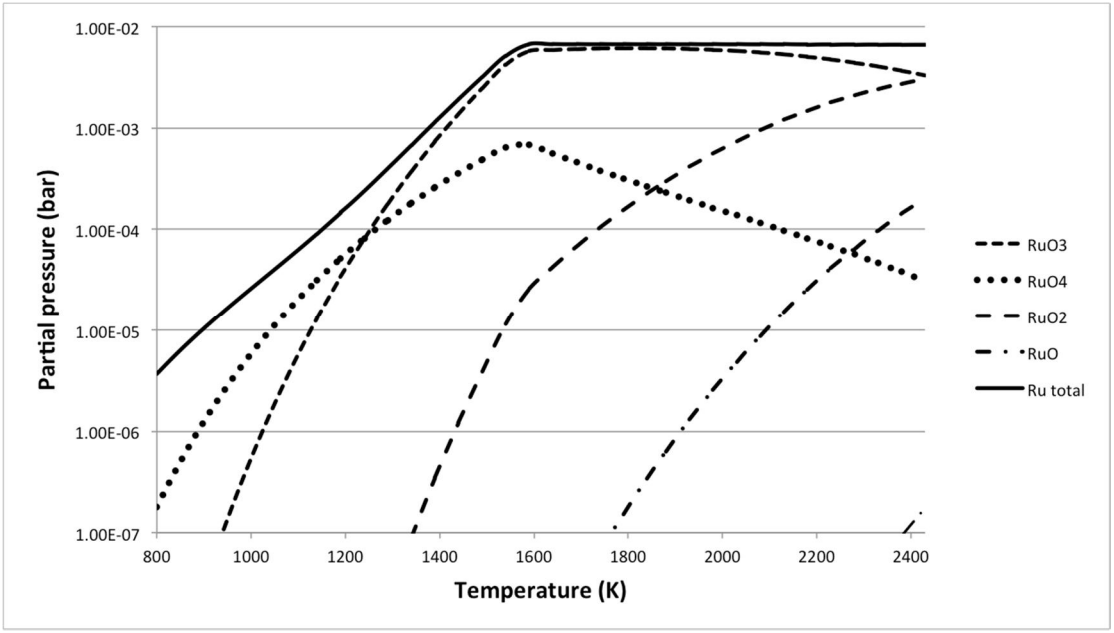

Figure 1. *Ruthenium gaseous species at thermodynamic equilibrium in air atmosphere at 1 bar pressure [4].*

Both gaseous RuO_2 and RuO_3 are unstable at lower temperatures, which makes their partial pressures in the gaseous atmosphere very low under 1000 K [5]. RuO_2 condenses

and RuO_3 decomposes into the form of solid RuO_2 according to the equations (1) and (2), in which K is the equilibrium constant [5]. Gaseous RuO_4 is also unstable at temperatures below 1000 K towards the decomposition to solid RuO_2, however its decomposition kinetics is much slower than in case of the other two oxides [6]. This makes RuO_4 the only relevant ruthenium gaseous species at temperatures below 1000 K.

$RuO_{2(g)} \rightarrow RuO_{2(s)}$ K=5E12 at 1000 K (1)

$2RuO_{3(g)} \rightarrow 2RuO_{2(s)}+O_{2(g)}$ K=3.7E12 at 1000 K (2)

The transport of ruthenium through a reactor cooling system (RCS) has been examined in few works before [7-9]. It was shown that the transport of ruthenium is affected by humidity, temperature and air flowrate in the RCS. Results indicate that ruthenium will be transported into the containment in two forms, aerosols consisting of anhydrous RuO_2 and gaseous RuO_4.

The interaction with other chemical elements released from the fuel may also affect the chemical form and possibly the quantity of transported ruthenium [10]. However, only a few experiments on ruthenium transport have dealt with atmospheric composition other that dry or humid air[11-13]. The use of pure air atmosphere to simulate air ingress conditions can be oversimplified in case of an accident due to the occurrence of aerosols (e.g. fission products, control rod materials) and various gaseous compounds produced by radiolysis of air [1, 14].

The main air radiolysis products present in the containment in the case of a severe accident are O_3, and nitrogen oxides, such as NO_2 and N_2O, which all have oxidizing properties [15]. Reaction of NO_2 with water leads also to the production of nitric acid (HNO_3). In case of air ingress these products may be able to oxidize the lower oxides of ruthenium (RuO_2, RuO_3) to RuO_4 in the reactor circuit and thus possibly increase the release and transport of gaseous ruthenium from the fuel [15]J. The reactions leading to the oxidation of lower ruthenium oxides into the form of volatile RuO_4, calculated with the HSC 5.11 chemistry software, are presented in equations (3-8) with the corresponding equilibrium constants[16].

$RuO_{3(g)}+NO_{2(g)} \leftrightarrow RuO_{4(g)}+NO_{(g)}$ K=16.8 at 1500 K (3)

$RuO_{3(g)}+2N_2O_{(g)} \leftrightarrow RuO_{4(g)}+2N_{2(g)}$ K=9.5E5 at 1500 K (4)

$3RuO_{3(g)}+2HNO_{3(g)} \leftrightarrow 3RuO_{4(g)}+2NO_{(g)}+H_2O_{(g)}$ K=4.5E10 at 1500 K (5)

$RuO_{2(s)}+2NO_{2(g)} \leftrightarrow RuO_{4(g)}+2NO_{(g)}$ K=2.8 at 1500K (6)

$RuO_{2(s)}+2N_2O_{(g)} \leftrightarrow RuO_{4(g)}+2N_{2(g)}$ K=9.0E9 at 1500 K (7)

$1.5RuO_{2(g)}+2HNO_{3(g)} \leftrightarrow 1.5RuO_{4(g)}+2NO_{(g)}+H_2O_{(g)}$ K=4.5E7 at 1500 K (8)

For a more precise and realistic modelling of the ruthenium chemistry in primary circuit conditions, experiments regarding aerosols and air radiolysis products interaction with Ru oxides in the gas phase are needed. Thus to provide a better insight into the chemistry of ruthenium during the transport through the RCS, the effect of nitrogen compounds (NO_2, N_2O, HNO_3) on the transport and speciation of ruthenium was examined in this work.

2. Experimental

2.1. Experimental facility and procedure

The configuration of "VTT´s Ru transport facility" for the experiments can be seen in Figure 2. The detailed description of the facility is given in the previous work [13]. The main component of the facility was the horizontal, tubular flow furnace (Entech, ETF20/18-II-L), which was used to heat the anhydrous RuO_2 powder (99.95 %, Alfa Aesar). The furnace was 110 cm long and it had two heating sections, each 40 cm long. These zones were separated by a 38 mm layer of insulation. At both ends of the furnace, there was 131 mm of thermal insulation. The furnace tube was made of high purity alumina (Al_2O_3, 99.7 %) and its inner diameter was 22 mm. The alumina crucible (length 20 cm) with the RuO_2 powder (mass. 1 or 2 g depending on the temperature used in the experiment) was placed in the beginning of the second heated zone of the furnace. As a new feature in these experiments, inside the furnace tube was inserted a second alumina tube (Al_2O_3, 99.7 %, outer diameter 6 mm with a wall thickness of 1 mm), which outlet was located directly after the crucible. The RuO_2 powder was heated to 1300 K, 1500 K or 1700 K in an oxidizing flow in order to produce gaseous ruthenium oxides.

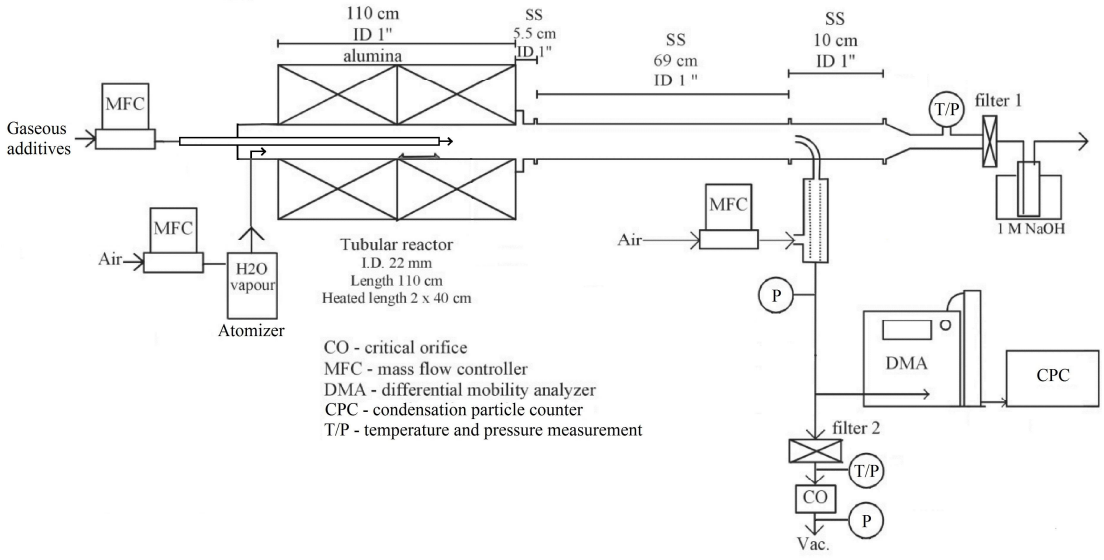

Figure 2. *Schematics of the experimental facility for ruthenium transport studies.*

The total flow rate through the facility was 5.0±0.1 l/min (NTP; NTP conditions 0 °C, 101325 Pa, measured with Thermal Mass Flowmeter TSI 3063, TSI Incorp.). Half of the total flow was directed through the inner furnace tube and the rest of the flow was passing through the furnace tube. The pressure inside the facility ranged from 102 to 104 kPa. The air flow (2.5±0.1 l/min, NTP) directed to the furnace tube was fed through an atomizer (TSI 3076). The air flow transported the water droplets (Milli-Q, ultrapure water, resistivity of 18.2 MΩ·cm at 25 °C) produced by atomizer via the heated line (120 °C) into the inlet of the furnace. Water evaporated when the droplets were heated and thus it led to an increase in the steam concentration within the furnace. A flow of N_2O, NO_2 or HNO_3 gases (2.5±0.1 l/min, NTP) was fed through the inner furnace tube. NO_2 was diluted with N_2 to obtain a similar concentration of precursor as in case of N_2O. As HNO_3 was fed with an additional atomizer (located then before the inlet of inner furnace tube, not presented in Figure 2), a carrier gas of nitrogen was used to transport HNO_3 droplets (solution of HNO_3 and Milli-Q water) via the heated line (120 °C) into the inlet of the inner furnace tube. The experimental matrix is presented in Table 1. The duration of experiments was 60 minutes for the experiments conducted in the humid air atmosphere (experiments 1 to 3) and 20 minutes for the experiments with additive precursors fed into the humid air atmosphere (experiments 4 to 12).

Table 1. *The detailed experimental matrix.*

Exp	T [K]	Gas[a]	Precursor	Additive precursor conc.	Humidity[b,c] [ppmV]
1	1300±12	Air	1g RuO_2	-	4.2E4/2.1E4
2	1500±12	Air	1g RuO_2	-	4.2E4/2.1E4
3	1700±12	Air	2g RuO_2	-	4.1E4/2.0E4
4	1300±12	Air+NO_2	1g RuO_2	50 ppmV NO_2	4.2E4/2.1E4
5	1500±12	Air+NO_2	1g RuO_2	50 ppmV NO_2	4.2E4/2.1E4
6	1700±12	Air+NO_2	2g RuO_2	50 ppmV NO_2	4.2E4/2.1E4
7	1300±12	Air+N_2O	1g RuO_2	50 ppmV N_2O	4.2E4/2.1E4
8	1500±12	Air+N_2O	1g RuO_2	50 ppmV N_2O	4.2E4/2.1E4

9	1700±12	Air+N_2O	2g RuO_2	50 ppmV N_2O	4.2E4/2.1E4
10	1300±12	Air+HNO_3	1g RuO_2	5 ppmV HNO_3	4.2E4/8.3E4
11	1500±12	Air+HNO_3	1g RuO_2	5 ppmV HNO_3	4.2E4/8.4E4
12	1700±12	Air+HNO_3	2g RuO_2	5 ppmV HNO_3	4.1E4/8.3E4

[a]*The total flow rate through the furnace over the crucible, before the inner tube outlet, was (2.5±0.1) l/min (NTP) and (5±0.1) l/min (NTP) after the inner tube outlet in every experiment.*

[b]*The humidity in the gas flow originated from the water based precursor solution of the atomizer.*

[c]*The humidity concentration is stated before/after the inner tube outlet. The increase of humidity in HNO_3 experiments is due to the water evaporation from the HNO_3 solution injected into the inner tube.*

After the vaporization of Ru and the following reactions within the gaseous atmosphere, the gaseous and particulate reaction products were trapped in a NaOH solution and collected on planer filters, respectively. Further details are given in [13]. Particles were also analysed online, see details below.

2.2. Analysis methods

2.2.1. Ruthenium release

The release rate of ruthenium during the experiments was obtained by weighting the mass of the crucible containing RuO_2 before and after the experiments. The mass of released RuO_2 was then converted to the corresponding mass of elemental ruthenium. Based on the previous study performed with the facility using ^{103}Ru radiotracer [7], the release of ruthenium from the crucible was assumed to be linear during the experiment.

2.2.2. Online analysis of ruthenium transport

The number size distribution of particles was measured online with a combination of a differential mobility analyser (DMA, TSI 3080/3081) and a condensation particle counter (CPC, TSI 3775) with a time resolution of 3 minutes. The flow rate through the devices was (0.30±0.01) l/min (NTP). The particles were size classified according to their electrical mobility by the DMA and the number of particles in each size classes was counted by the CPC (with a counting efficiency higher than 96%). The measurement range was from 15 nm to 670 nm. However, a pre-impactor removed particles larger than 615 nm at the inlet of the DMA. The measurement system was controlled with the

Aerosol Instrument Manager software version 9.0 (TSI). This measurement system is called as Scanning Mobility Particle Sizer (SMPS).

All the presented online measurement data was corrected considering the loading of analysis filter by particles and the following decrease in the flow rate through the filter and thus the decreased flow rate into the aerosol sampling line from the main line. The correction was based on the calibration of flow rate through the critical orifice (CO) at various temperatures and pressures simulating the loading of filter. The calibration data was then utilized to estimate the flow rate of CO in the experiments with the help of temperature and pressure measurement data. Also the flow rate from the main line to the aerosol line was always measured with Thermal Mass Flowmeter at the beginning of every experiment. As a result, the changes in dilution ration could be taken into consideration. The highest uncertainty in the dilution ratio originated from the inaccuracy of mass flow controller feeding air through the porous tube dilutor and of Thermal Mass Flowmeter. Given that the uncertainty of both devices can be ±2% of the reading, the uncertainty in the dilution ratio was ca. ±4%. Otherwise the contribution of uncertainties in temperature and pressure measurements on the dilution ratio was low, since the flow rate through the critical orifice did not vary significantly due to these uncertainties. The presented online data was also depended on the flow rate through the main line. The flow rate was always measured in the beginning of experiments, thus an additional uncertainty of ±2% was resulted from the flowmeter. Therefore, the combined conservative uncertainty estimate for the presented online data was ca. ±6%. The particle number concentration values measured with CPC were also up to 4% too low due to the deficiency in counting efficiency.

2.2.3 Intrumental Neutron Activation Analysis (INAA)

The quantification of ruthenium aerosols collected on filters and gaseous ruthenium trapped in the sodium hydroxide liquid traps was done by use of INAA (Instrumental Neutron Activation Analysis). Ruthenium in the liquid traps was precipitated with addition of EtOH (96% Sigma-Aldrich), centrifuged and then filtered from the solution. Aerosols collected on the PTFE filters were used as they were after the experiment. Samples were then irradiated in the research reactor at VTT (Triga mark II reactor in Otaniemi, Espoo). Irradiations were done with a thermal neutron flux of $8.7 \cdot 10^{12}$ n·cm^{-2}·s^{-1} and epithermal flux of $4.6 \cdot 10^{12}$ n·cm^{-2}·s^{-1}. Samples were irradiated from 10 minutes up to 4 hours dependable on ruthenium content in the sample. After one week of cooling time, the samples were measured by means of gamma spectrometry.

For the measurements High Purity Germanium (HPGe) detector (Ortec model GEM-15180-S) was used with a relative efficiency 17.7% and resolution of 1.7keV both at 1332 keV. The evaluation of data was done with GammaVision software version 7.01.03. (Ortec). The detector was empirically calibrated for both energy and efficiency with QCYA18189 (Eckert & Ziegler) standard radionuclide source solution with the same geometry as irradiated samples.

The activity of ^{103}Ru was determined from counts at 497keV peak where absolute efficiency at given geometry was determined to be 1.7%. The detection limit for ruthenium was determined to be 1.0E-2 µg based on the times of irradiations and measurements. Uncertainty of the measurements was calculated to be 5% according to GUM (the Guide to the Expression of Uncertainties in Measurements)[17].

2.3. Chemical characterisation

2.3.1 X-ray photoelectron spectroscopy

Chemical analysis of the collected aerosol samples was done using a XPS (X-ray photoelectron spectroscopy. With use of XPS elemental composition of the samples as well as oxidation states of detected elements was determined. For the XPS measurements Perkin Elmer Phi 5500 Multi Technique System was used. The detailed setup of the machine during measurements was described in the previous work [18]. Commonly, C 1s peak is used as an internal standard for the binding energies during XPS measurements. In the case of ruthenium Ru 3d5/2 peak is overlapping with C 1s peak what makes this reference unreliable, thus gold foil conductively connected to the measured samples was used as an internal standard during the measurements. The experimental uncertainty of binding energy of Ru $3d_{5/2}$ peak was determined to be ±0.1 eV. The collected spectra were curve fitted with PHI Multipak software (Ulvac-Phi inc.) assuming Shirley background. The asymmetrical shape of peaks was used due to the conductive nature of anhydrous RuO_2 [19]. XPS analysis was performed from at least two different spots on the samples.

2.3.2. X-ray diffraction analysis (XRD)

Crystalographic structure of the collected aerosols was examined by means of XRD (X-ray diffraction analysis). The combination of XPS and XRD analysis allowed the characterization of both crystalline and eventually amorphous compounds in the collected aerosols. XRD measurements were performed using Bruker D2 Phaser diffractometer with Cu Kα characteristic radiation, equipped with scintillation detector. Rotation speed of the sample holder was 360°/min and measurement angle interval was 20-80° 2-theta. The comparison of the obtained data with standards in the Joint Committee of Powder Diffraction Standards database [20] led to the identification of compounds.

3. Results

3.1. Release and transport results

3.1.1. Release of ruthenium

The release of ruthenium from the crucible was analyzed by weighting the crucible with RuO_2 precursor before and after the experiment. The release rate results are presented in Table 2.

Table 2. *Release rates of ruthenium from the crucible*

Experiment	Ruthenium release mg/min
1. Air (1300 K)	0.34±0.02
2. Air (1500 K)	3.22±0.16
3. Air (1700 K)	20.27±1.04

The release rate of ruthenium from the crucible was fairly similar in all the experiments conducted at the same temperature. As the location of additional precursors injection into the airflow was just after the crucible, the precursors were not affecting the vaporization of ruthenium and the observed ruthenium release results could be expected. When compared with the previously performed experiments, the decrease in airflow over the crucible from 5.0 l/min to 2.5 l/min resulted into a decrease in the release rate of ruthenium approximately by half [7, 13]. This effect can be attributed to the lower absolute amount of oxygen reaching the ruthenium in the crucible.

3.1.2. Ruthenium transport

The quantification of ruthenium transport in forms of aerosols collected on the filters and gaseous ruthenium retained in the 1M NaOH traps was done with use of INAA (Instrumental Neutron Activation Analysis). The fractions of ruthenium transported in forms of gas and aerosols through the model primary circuit in all experiments are presented in Table 3. The values are given as % of the released ruthenium. In all experiments significant amount of ruthenium was visually observed to be deposited at the outlet of the furnace, where the temperature gradient was the highest. Similar behavior was also detected in the previous work with the same facility [21]. The effects of different precursors and temperature on the transport of ruthenium are further discussed in the following chapters.

Table 3. *The fractions of ruthenium transported as RuO_2 aerosol particles and RuO_4 gas through the model primary circuit and the fraction of ruthenium deposited inside the circuit. The values are given as % of the released ruthenium. The uncertainties are given as 2 standard deviations.*

Exp. [#]	Ru transported in total (%)	RuO_2 transported (%)	RuO_4 transported (%)	Ru deposited (%)
1 (1300 K)	9.3±0.9	9.1±0.5	0.024±0.012	90.7±1.4
2 (1500 K)	12.8±1.3	12.8±0.6	0.010±0.005	87.2±1.9
3 (1700 K)	14.3±1.4	14.3±0.7	0.00±0.005	85.7±2.0
4 (NO_2 1300 K)	13.9±1.4	0.010±0.005	13.9±0.7	86.1±2.0
5 (NO_2 1500 K)	13.9±1.4	4.0±0.2	9.9±0.5	86.1±2.0
6 (NO_2 1700 K)	20.2±2.0	20.2±1.0	0.00±0.005	79.8±3.1
7 (N_2O 1300 K)	6.1±0.6	6.0±0.3	0.13±0.01	93.9±1.0
8 (N_2O 1500 K)	25.5±2.6	25.4±1.7	0.14±0.01	74.5±3.8
9 (N_2O 1570 K)	15.5±1.6	15.5±0.8	0.00±0.005	84.5±2.3
10 (HNO_3 1300 K)	10.4±1.0	9.1±0.5	1.2±0.1	89.7±1.6
11 (HNO_3 1500 K)	13.1±1.3	11.8±0.6	1.3±0.1	86.9±2.0
12 (HNO_3 1700 K)	14.4±1.4	13.6±0.7	0.78±0.04	85.7±2.2

3.1.2.1. Air atmosphere

The ratio between ruthenium transported as gas and as aerosols in the humid air atmosphere was determined and it is presented in Table 4. From the data it can be seen that ruthenium in form of aerosols was predominating over RuO_4 within the whole temperature interval of experiments (1300 K – 1700 K). With the increasing temperature the gaseous fraction was decreasing with respect to the aerosol one. This is in agreement with the trend in thermodynamic equilibrium calculations performed with the HSC 5.11. software [16]. The overall transport of ruthenium was also promoted with

the increasing temperature. It is also noticeable that when compared with the previous experiments [13] the transported ruthenium gaseous fraction was lower. This indicates the effect of the flow rate on the transport of RuO_4 through the RCS. Similar effect has been observed in a previous study with very low flow rates used in the experiments [9].

Table 4. *Mass of ruthenium transported as aerosol particles and as gas through the model primary circuit under humid air atmosphere. The uncertainties are given as 2 sigma standard deviation.*

Exp. [#]	Ru transported in total (mg)	Ru in form of RuO_2 aerosol (mg)	Ru in form of RuO_4 gas (mg)	Ratio of RuO_2/ RuO_4	Ru deposited inside the facility (mg)
1. (1300 K)	0.64±0.01	0.62±0.001	0.020±0.001	38±1	8.4±0.1
2. (1500 K)	8.3±0.4	8.3±0.4	0.010±0.001	1636±40	76.7±0.8
3. (1700 K)	57.9±2.9	57.9±2.9	0.001±0.001	1.25E5± 3.1E3	475.8±4.8

3.1.2.2. Atmosphere with 50 ppmV of NO_2

The results of ruthenium transport under humid air atmosphere with 50 ppmV of NO_2 additive are presented in Table 5. The feed of NO_2 into the airflow affected the composition of transported ruthenium resulting into a higher transport of gaseous RuO_4 through the facility.

Table 5. *Mass of ruthenium transported as aerosol particles and as gas through the model primary circuit under humid air atmosphere with 50 ppmV of NO_2. The uncertainties are given as 2 sigma standard deviations.*

Exp. [#]	Ru transported in total (mg)	Ru in form of RuO_2 aerosol (mg)	Ru in form of RuO_4 gas (mg)	Ratio of RuO_2/ RuO_4	Ru deposited inside the facility (mg)
4. (1300 K)	1.23±0.07	0.000± 0.001	1.23±0.07	0.0010± 0.0003	10.37±0.14
5. (1500 K)	8.96±0.45	2.55±0.13	6.40±0.32	0.40±0.01	76.04±2.2
6. (1700 K)	82.01±4.10	82.00± 4.10	0.010± 0.005	13231±330	451.66±8.3

The strong effect of temperature on the transported ruthenium species was observed. This behaviour was attributed to two different phenomena. The first one was the thermal decomposition of NO_2 [22] according to reaction (9) [23].

$2NO_{2(g)} \leftrightarrow O_{2(g)}+2NO_{(g)}$ with $k = 1.5 \times 10^{13} \exp(-654OO/RT)$ $mol^{-1}.sec^{-1}$ (9)

The second was the decreasing ability of the NO_2 to oxidize RuO_3 to RuO_4 according to reaction (10) with increasing temperature. As a result, the NO_2 injection into the gas flow increased the amount of transported gaseous ruthenium in the experiments with temperatures of 1300 K and 1500 K. The corresponding aerosol fraction decreased significantly. When temperature was increased to 1700 K, the transport of ruthenium in aerosol form increased strongly and the transport of gaseous ruthenium was very low. The equilibrium constants for this reaction (10) were calculated with the HSC 5.11. software[16] and they are presented in Table 6. The ratios between aerosol and gaseous fraction of transported ruthenium are lower than thermodynamic equilibrium calculations predict.

$$RuO_{3(g)}+NO_{2(g)} \leftrightarrow RuO_{4(g)}+NO_{(g)} \qquad (10)$$

Table 6. *Equilibrium constants for the oxidation of RuO_3 by NO_2 to RuO_4 at different temperatures.*

Temperature	K_{eq}
1300 K	28.55
1500 K	16.85
1700 K	11.3

As can be seen from Table (4) the absolute amount of transported ruthenium was increased when compared to the humid air atmosphere mainly under temperatures 1300 K and 1700 K with nearly 92 % and 49 % increase, respectively.

3.1.2.3. Atmosphere with 50 ppmV of N_2O

The effect of N_2O on the transport of ruthenium is summarized in Table 7. At all studied temperatures the injection of N_2O decreased the gaseous fraction of ruthenium transported through the facility when compared with the humid air experiments. This behavior was attributed to the reactions (11) and (12) and subsequent decomposition of RuO_3 into a solid RuO_2 at the outlet of the furnace where temperature decreased below 1000 K.

$$RuO_{4(g)}+N_2O_{(g)} \leftrightarrow RuO_{3(g)}+2NO_{(g)} \qquad (11)$$

$$RuO_{4(g)}+2N_2O_{(g)} \leftrightarrow RuO_{2(s)}+4NO_{(g)} \qquad (12)$$

Table 7. *Mass of ruthenium transported as aerosol particles and as gas through the model primary circuit under humid air atmosphere with 50 ppmV of N_2O. The uncertainties are given as 2 sigma standard deviation.*

Exp. [#]	Ru transported in total (mg)	Ru in form of RuO_2 aerosol (mg)	Ru in form of RuO_4 gas (mg)	Ratio of RuO_2/ RuO_4	Ru deposited inside the facility (mg)
7. (1300 K)	0.54±0.03	0.53±0.03	0.010±0.005	47.0±1.2	11.1±0.1
8. (1500 K)	16.5±0.1	16.4±0.82	0.090±0.005	177±4.4	68.5±0.9
9. (1700 K)	62.9±3.1	62.9±3.1	0.010±0.005	6123±153	470.8±3.1

The absolute transport of ruthenium through the facility decreased when compared to the humid air atmosphere at 1300K. The decrease was about 16%. On the other hand, at 1500K the mass of transported ruthenium was increased by a factor of 2 at the outlet of the facility when compared to the humid air atmosphere. At 1700 K the observed increase in Ru transport was modest. This is a noticeable effect predicting a higher ruthenium transport as aerosol through the primary circuit if N_2O is in the atmosphere.

3.1.2.4. Atmosphere with **5** ppmV of HNO_3

The results for ruthenium transport under the humid air atmosphere with 5 ppmV of HNO_3 are presented in Table 8. The injection of HNO_3 into the airflow affected the composition of transported ruthenium resulting into a higher transport of gaseous RuO_4 through the facility when compared to the pristine humid air atmosphere at all temperatures used in the experiments.

Table 8. *Mass of ruthenium transported as aerosol particles and as gas through the model primary circuit under humid air atmosphere with 5 ppmV of HNO_3. The uncertainties are given as 2 sigma standard deviation.*

Exp. [#]	Ru transported in total (mg)	Ru in form of RuO_2 aerosol (mg)	Ru in form of RuO_4 gas (mg)	Ratio of RuO_2/ RuO_4	Ru deposited inside the facility (mg)
10. (1300 K)	0.9±0.5	0.80±0.04	0.11±0.01	7.5±0.2	10.7±0.5
11. (1500 K)	8.5±0.4	7.6±0.4	0.86±0.04	8.8±0.2	76.5±0.5
12. (1700 K)	58.2±3.0	55.0±2.8	3.2±0.2	17.5±0.4	475.5±3.0

The effect of nitric acid injection was not as prominent as could be expected from the thermodynamic calculations indicating that K values for reaction (13) would be 1.65E11, 4.57E10 and 1.66E10 for temperatures 1300 K, 1500 K and 1700 K, respectively [16]. This can be again explained by the thermal decomposition of HNO_3 to the lower nitrogen oxides [24, 25] thus lowering the amount of precursor in the gas phase.

$$3RuO_{3(g)}+2HNO_{3(g)} \leftrightarrow 3RuO_{4(g)}+H_2O_{(g)}+2NO_{(g)} \quad (13)$$

As can be seen from Tables 8 and 4 the absolute amount of transported ruthenium was fairly similar when compared to the humid air atmosphere under all temperatures used in the experiments.

3.1.3. Online monitoring of aerosol transport

The transport of aerosol particles was monitored online in order to have information on the transient behavior of ruthenium in the facility. The properties of particles, such as number concentration, diameter and number size distribution, were measured with SMPS at the outlet of the facility. The range of measurement uncertainty ±10% in the experiments is not displayed in the figures 3 and 4 below. The data of experiment 10 is not presented due to a fault in the online measurement.

The evolution of particle number concentration and the count median diameter (CMD) of particles in the experiments is shown in Figure 3. The vaporization temperature of ruthenium inside the furnace had an obvious effect on the diameter of particles. The increase of temperature from 1300 K to 1700 K caused an increase of particle diameter in every experiment, resulting in up to 3.5 times larger particles in case of NO_2 feed. This phenomenon is directly connected to a higher release of ruthenium from the crucible and to the following formation of particles. High release of ruthenium also favors the agglomeration of particles, when the concentration of particles exceeds ca. 10^6 particles per cm^3 [26]. Contrary to the particle CMD, the number concentration of particles remained on a rather similar level in the experiments when only the effect of RuO_2 vaporization temperature was examined.

The feed of nitrogen compounds (NO_2, N_2O, HNO_3) into the flow of Ru oxides changed the transport of particles when compared with the reference experiments 1 to 3. In general, the number concentration of particles decreased, but at the same time the diameter of particles seemed to increase. Depending on the experiment, the particle CMD ranged from ca. 20 to 210 nm. In case of NO_2 feed, the measured particle concentration was at the lowest level ranging mainly from ca. 10^3 to 10^6 particles per cm^3 in experiments 4 and 5. The concentration increased in experiment 6 and it was observed to be between ca. 10^6 and 10^7 particles per cm^3. Furthermore, the particle diameter was the highest and it seemed to even increase strongly in the course of experiment. It indicated, in addition to the agglomeration of particles, that probably part of the formed gaseous Ru compounds were condensing on the surface of the existing particles and thus increased the particle diameter. This conclusion is also supported by

the measured low number concentration of particles and the previous observation on high formation of gaseous Ru due to NO_2, see[13].

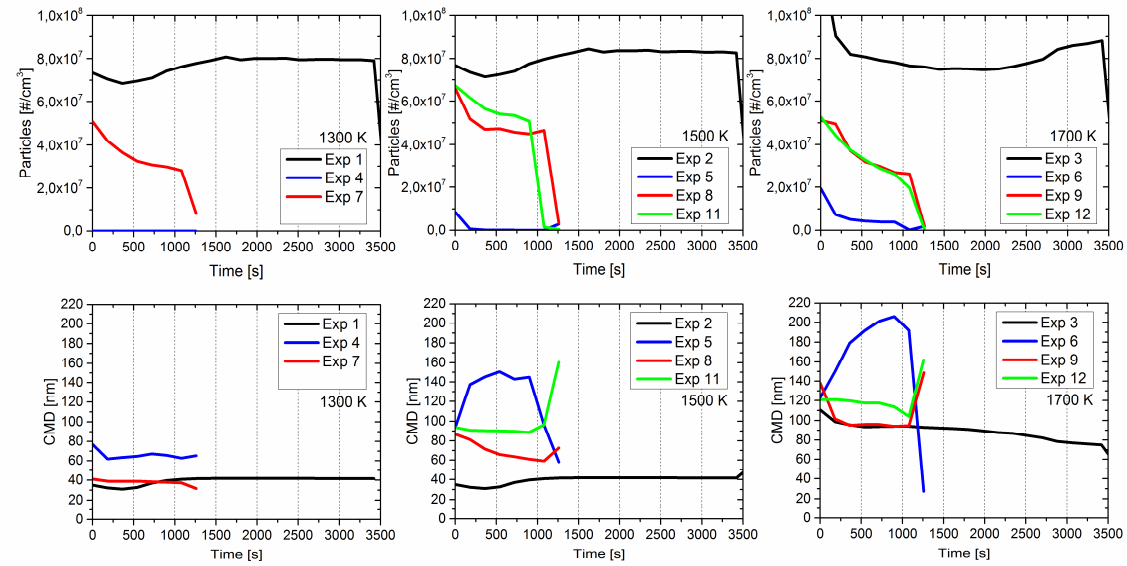

Figure 3. *The particle number concentration [#/cm³] (above) and count median diameter [nm] (below) at the outlet of the facility during experiments (measured with SMPS). The duration of experiments 1 to 3 was 60 minutes, whereas the rest of experiments lasted for 20 minutes.*

The particle number size distribution at the moment of 750 seconds since the beginning of experiment is presented in Figure 4. The data is presented for a particle diameter range from 15 to 500 nm. In addition to the above observations on particle behavior, it was noticed that the transported particles were lognormally distributed and most of the particles were smaller than 500 nm in diameter. The shape of the particle number size distribution did not vary a lot due to the feed of nitrogen compounds N_2O and HNO_3 in the studied conditions. The broad particle distribution and the emphasis of large particles (100 to 500 nm) in the distribution were evident when NO_2 was present in the atmosphere, see the case of 1700 K.

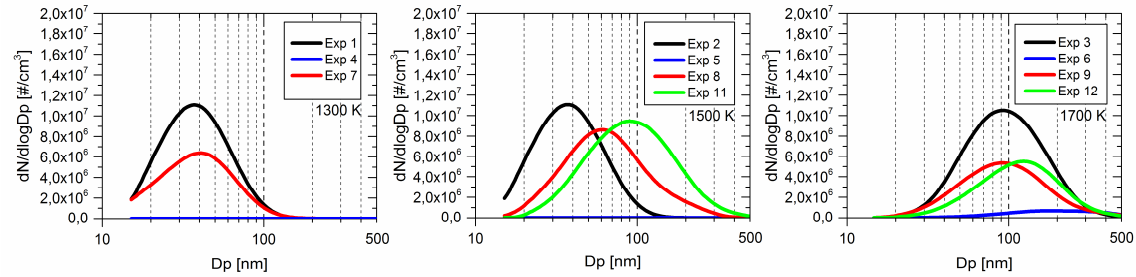

Figure 4. *The particle number size distribution at the moment of 750 seconds since the beginning of experiment (measured with SMPS).*

3.2. Chemical characterization

3.2.1. XPS analysis

The chemical speciation of aerosols particles transported through the facility and then collected on the PTFE filters was examined with XPS technique. The XPS measurements revealed the binding energies of electrons in the elements of interest thus identifying the chemical composition of the collected aerosols. The identification was based on the comparison between the identified binding energies of ruthenium on the samples with the reference binding energy values found in the literature. The reference samples of commercial ruthenium dioxide powders both anhydrous and hydrated (purity of 99.5%, Alfa Aesar) were analysed and the obtained spectra were then compared with the spectra of ruthenium containing samples.

The reference electron binding energy values of ruthenium used in this work are presented in Table 9. As it can be seen in the table, the binding energies are not only dependent on the oxidation state of ruthenium but also on its chemical environment, e.g. the hydration of RuO_2. Similar effect has also been observed in a previous study [27]. Thus, the comparison of all obtained spectra in the region of Ru 3d5/2 peak brings better insight into the chemical characterization of the measured ruthenium compound.

The binding energies for Ru 3d5/2 peak in all samples were within the region of 280.4 eV-280.5 eV as it can be seen in Figure 5. It indicates, that the transported ruthenium aerosols were in the form of anhydrous RuO_2 in all experimental conditions. Also the overall characteristics of spectra are very similar to each other, which strengthen the assumption that all spectra are originating from the same compound.

It should be pointed out that nitrogen was not detected in the collected samples, thus the possible formation of ruthenium nitrosyl compounds [28, 29] was ruled out during the data evaluation process.

Table 9. *Reference values for the electron binding energies of various ruthenium compounds.*

Compound	Binding energy for Ru 3d 5/2 line (eV)
RuO_2	280.5[18]
$RuO_2 \cdot H_2O$	282.1[18]
RuO_4	283.3[30]
$BaRuO_4$	284.2[31]
$RuCl_3$	282.1[31]
Ru (metal)	280.0[30]

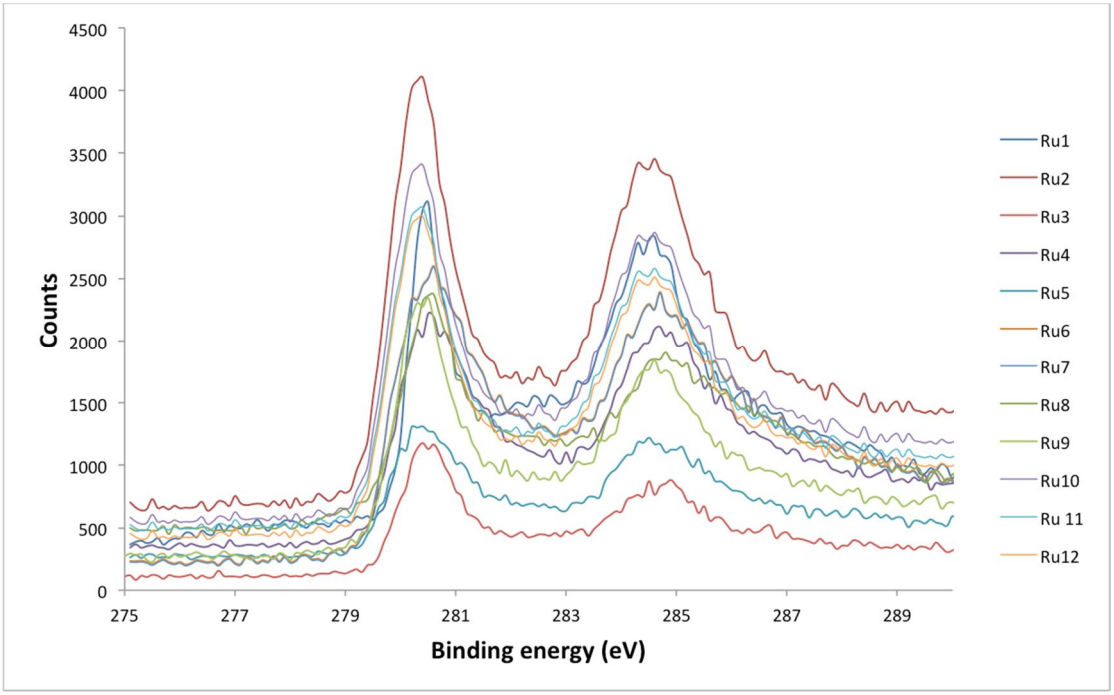

Figure 5. *The obtained XPS spectra from the analysis of collected aerosols on filters.*

3.2.2. XRD

The results from the qualitative crystallographic X-ray diffraction analysis of the samples are shown in Figure 6. The recorded XRD spectra in experiments 1 to 9 have shown the same diffraction pattern, which corresponds to the rutile structure of RuO_2. This is in a good agreement with the XPS analysis leading to the conclusion that aerosols collected from the gas flow were in a form of anhydrous ruthenium dioxide.

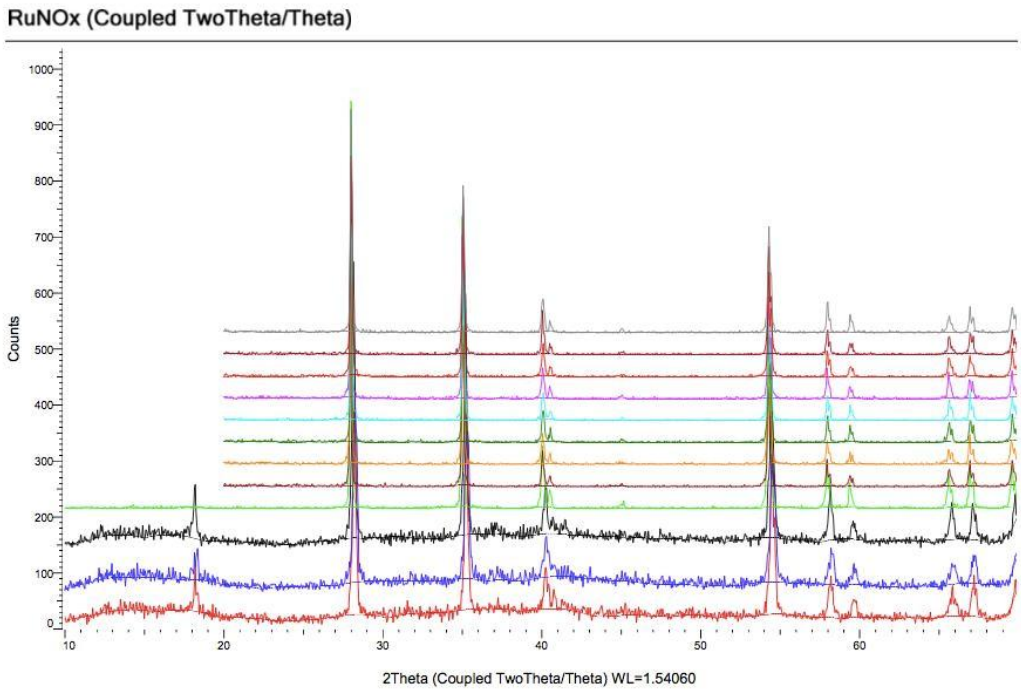

Figure 6. *The obtained XRD spectra from the samples of experiments 1 to 12. The height of the peaks was scaled in order to fit in the figure.*

4. Conclusions

The focus in this study was to reveal the effect of different nitrogen oxides and nitric acid on the transport and chemical composition of ruthenium in the model primary circuit heated up to 1300 K, 1500 K or 1700 K simulating an air ingress accident. The main focus was on the quantification of the gaseous and solid fractions of ruthenium transported through the circuit, in which temperature decreased to ca. 300 K.

In the performed experiments, the effects of humid air, NO_2, N_2O and HNO_3 on the transport and partitioning of ruthenium were investigated. Nitrogen oxides and nitric acid were used as representatives of the air radiolysis products formed in the gas phase during a nuclear accident.

The release rate of ruthenium (given as for elemental Ru) from the RuO_2 powder precursor was determined to be dependable on the temperature with values of (0.34±0.07) mg/min at 1300 K, (3.22±0.16) mg/min at 1500 K and (20.27±1.04) mg/min at 1700 K under air atmosphere with a low content of steam (≈2.1E4 ppmV).

The partitioning of ruthenium was examined by collecting aerosol particles on a PTFE filter and trapping gaseous RuO_4 into 1M NaOH solution traps. During experiments the majority of ruthenium was deposited inside of facility. In visual examination, the deposition was detected mainly at the outlet of the furnace where the temperature gradient was the highest.

The quantification of ruthenium transport showed a significant impact of the experimental conditions on both the absolute amount as well as on the partitioning of the transported ruthenium between gaseous and aerosol compounds. In general, the increase in temperature resulted in a higher release of ruthenium from the precursor and also to a higher transport of ruthenium.

In case of 50 ppmV of NO_2 in the humid air flow, a major effect on the fractions of gaseous and solid ruthenium was identified. The gaseous fraction of transported ruthenium was significantly increased under all temperatures due to NO_2. At temperatures of 1300 K and 1700 K the overall transport of ruthenium was significantly increased when compared to the humid air atmosphere. The diameter of particles seemed to increase in the course of experiments, whereas the particle number concentration was low. It is suggested, that part of the formed gaseous Ru compounds was condensing on the surface of the existing particles and thus increased the particle diameter.

Introduction of 50 ppmV of N_2O into the gas phase led to a decrease of RuO_4 transport through the facility as well as to an increased fraction of ruthenium transported in form of aerosols. Nearly 100% increase in the total amount of transported ruthenium was detected at temperature of 1500 K when compared to the humid air atmosphere.

An interesting observation was also done in the experiments with 5 ppmV of HNO_3 in the humid air flow. The transport of gaseous ruthenium increased at all studied

temperatures. However, the overall transport of ruthenium was fairly similar than in humid air atmosphere.

The analysis of chemical speciation of the transported aerosols by XPS and XRD methods showed that the chemical form of aerosols was anhydrous RuO_2.

The results obtained in this study showed significant effect of nitrogen oxides as well as nitric acid on the transport and speciation of ruthenium in primary circuit conditions. This indicates a possible increase in the fraction of gaseous ruthenium reaching the containment building during a severe nuclear accident in case of air ingress and entry of NO_2 and HNO_3 into the reactor. The obtained data bring additional insight into the ruthenium chemistry during a nuclear accident and reveal the possible interactions of ruthenium with the air radiolysis products. This information will help to improve the modeling of ruthenium behavior under severe nuclear accident conditions and enhance the nuclear safety.

Acknowledgements

This study was performed as part of Nordic collaboration, ATR-2 (Impact of Aerosols on the Transport of Ruthenium) experimental programme, between Finland and Sweden. The financial support of SAFIR 2018, APRI 9 and NKS-R programmes is acknowledged.

References

1. Haste, T., F. Payot, and P.D.W. Bottomley, *Transport and deposition in the Phébus FP circuit.* Annals of Nuclear Energy, 2013. 61(0): p. 102-121.

2. Grégoire, A.C. and T. Haste, *Material release from the bundle in Phébus FP.* Annals of Nuclear Energy, 2013. 61: p. 63-74.

3. Ducros, G., Y. Pontillon, and P.P. Malgouyres, *Synthesis of the VERCORS experimental programme: Separate-effect experiments on Fission Product release, in support of the PHEBUS-FP programme.* Annals of Nuclear Energy, 2013. 61(0): p. 75-87.

4. Bale, C., P. Chartrand, S.A. Degterov, G. Eriksson, K. Hack, R. Ben Mahfoud, J. Melancon, A.D. Pelton, and S. Petersen, *FactSage thermochemical software and databases.* Calphad-Computer Coupling of Phase Diagrams and Thermochemistry, 2002. 26(2): p. 189-228.

5. Eichler, B., F. Zude, W. Fan, N. Trautmann, and G. Herrmann, *Volatilization and Deposition of Ruthenium Oxides in a Temperature Gradient Tube.* Radiochimica Acta, 1992. 56(3): p. 133-140.

6. Mun, C., L. Cantrel, and C. Madic, *Study of RuO4 decomposition in dry and moist air.* Radiochimica Acta, 2007. 95(11): p. 643-656.

7. Kärkelä, T., Backman, U., Auvinen, A., Zilliacus, R., Lipponen, M., Kekki, T., Tapper U., Jokiniemi, J., *, Experiments on the behaviour of ruthenium in air ingress accidents - Final report*. 2007, VTT research report - VTT-R-01252-07

8. Kärkelä, T., N. Vér, T. Haste, N. Davidovich, J. Pyykönen, and L. Cantrel, *Transport of ruthenium in primary circuit conditions during a severe NPP accident.* Annals of Nuclear Energy, 2014. 74(0): p. 173-183.

9. Vér, N., L. Matus, A. Pintér, J. Osán, and Z. Hózer, *Effects of different surfaces on the transport and deposition of ruthenium oxides in high temperature air.* Journal of Nuclear Materials, 2012. 420(1–3): p. 297-306.

10. Di Lemma, F.G., J.Y. Colle, O. Beneš, and R.J.M. Konings, *A separate effect study of the influence of metallic fission products on CsI radioactive release from nuclear fuel.* Journal of Nuclear Materials, 2015. 465: p. 499-508.

11. Backman, U., Lipponen, M., Auvinen, A., Jokiniemi, J., Zilliacus, R.,, *Ruthenium Behaviour in Severe Nuclear Accident Conditions - Final Report,* in *VTT research report PRO3/P27/04*. 2004.VTT research report PRO3/P27/04,

12. Backman, U., M. Lipponen, A. Auvinen, U. Tapper, R. Zilliacus, and J.K. Jokiniemi, *On the transport and speciation of ruthenium in high temperature oxidising conditions.* Radiochimica Acta, 2005. 93(5): p. 297-304.

13. Kajan Ivan, Kärkelä Teemu, Tapper Unto, Johansson Leena-Sisko, Gouëllo Mélany, Ramebäck Henrik, Holmgren Stina, Auvinen Ari, Ekberg Christian, *Impact of Ag and NOx compounds on the transport of ruthenium in the primary circuit of nuclear power plant in a severe accident.* Submited to: Annals of Nuclear Energy, 2016.

14. Bosland, L., F. Funke, G. Langrock, and N. Girault, *PARIS project: Radiolytic oxidation of molecular iodine in containment during a nuclear reactor severe accident: Part 2. Formation and destruction of iodine oxides compounds under irradiation – Experimental results modelling.* Nuclear Engineering and Design, 2011. 241(9): p. 4026-4044.

15. Mun, C., L. Cantrel, and C. Madic, *Review of literature on ruthenium behavior in nuclear power plant severe accidents.* Nuclear Technology, 2006. 156(3): p. 332-346.

16. *HSC Chemistry for Windows, version 5.11.* . 2002, Outokumpu Research Oy; Pori, : Finland

17. Metrology, B.J.C.f.G.i., *JCGM 100:2008, Evaluation of measurement data – Guide to the expression of uncertainty in measurement JCGM 100:2008 (GUM 1995 with minor corrections).* . 2008: Paris

18. Kajan, I., *RuO4 interaction with surfaces in the containment of nuclear power plant,* in *Nuclear chemistry*. 2014, Chalmers University of Technology.ISSN 1652-943X,

19. Mun, C., J. Ehrhardt, J. Lambert, and C. Madic, *XPS investigations of ruthenium deposited onto representative inner surfaces of nuclear reactor containment buildings.* Applied Surface Science, 2007. 253(18): p. 7613-7621.

20. *JOINT COMMITTEE ON POWDER DIFFRACTION STANDARDS.* Analytical Chemistry, 1970. 42(11): p. 81A-81A.

21. Kärkelä, T., Pyykönen, J., Auvinen, A., Jokiniemi, J., *Analysis of Flow Fields, Temperatures and Ruthenium Transport in the Test Facility*. 2008, VTT Technical Research Centre of Finland: Espoo, Finland

22. Polanyi, J.C., *Erratum: Isotopic Reaction Rates Between Methyl and Hydrogen.* The Journal of Chemical Physics, 1956. 24(2): p. 493-493.

23. Huffman, R.E. and N. Davidson, *Shock Waves in Chemical Kinetics: The Thermal Decomposition of NO21a.* Journal of the American Chemical Society, 1959. 81(10): p. 2311-2316.

24. Harrison, H., H.S. Johnston, and E.R. Hardwick, *Kinetics of the Thermal Decomposition of Nitric Acid Vapor. IV. A Shock Tube Study Between 800-1200°K.* Journal of the American Chemical Society, 1962. 84(13): p. 2478-2482.

25. Ellis, W.R. and R.C. Murray, *The thermal decomposition of anhydrous nitric acid vapour.* Journal of Applied Chemistry, 1953. 3(7): p. 318-322.

26. Hinds, W.C., *Aerosol technology: properties, behavior, and measurement of airborne particles*. Vol. 2. 1999, New York: Wiley.

27. Holm, J., Glänneskog, H., Ekberg, Ch.,, *Deposition of RuO4 on various surfaces in a nuclear reactor containment.* Journal of Nuclear Materials, 2009. 392: p. 55-62.

28. Fletcher, J.M., I.L. Jenkins, F.M. Lever, F.S. Martin, A.R. Powell, and R. Todd, *Nitrato and nitro complexes of nitrosylruthenium.* Journal of Inorganic and Nuclear Chemistry, 1955. 1(6): p. 378-401.

29. Sasahira, A. and F. Kawamura, *Formation Rate of Ruthenium Tetroxide during Nitric Acid Distillation.* Journal of Nuclear Science and Technology, 1988. 25(7): p. 603-606.

30. Kim, K.S. and N. Winograd, *X-Ray Photoelectron Spectroscopic Studies of Ruthenium-Oxygen Surfaces.* Journal of Catalysis, 1974. 35(1): p. 66-72.

31. Ohyoshi, A., F. Götzfried, and W. Beck, *Polynuclear carbonyl complexes of ruthenium and osmium with methylthiolate and bromine bridging ligands.* Chemistry Letters, 1980. 9(12): p. 1537-1540.